5.6 Longitudinal and Lateral Damping Mechanisms

The definition of a damping mechanism which is applicable to mine hoist cables has not received a great deal of attention, probably due to the complexity and variation of the rope construction. Mankowski [1986],[1988],[1990] has provided the bulk of the fundamental work in the specific area of mine hoist cables, whilst earlier work by Yu [1952] and Vanderveldt et al [1973] examined some of the parameters influencing the damping characteristics of wire ropes.

5.6.1 Longitudinal Damping

Usually a visco-elastic damping model is applied in the mining industry to study longitudinal oscillations of the mine hoist system. Since these works are concerned primarily with the start up transients, which exhibit dominant first mode response, the damping model is formulated with respect to the measurement of the logarithmic decrement of the first longitudinal mode. Thomas et al.[1987] performed such measurements at Deelkraal Mine with an empty and loaded skip, at $\frac{1}{4}$ and $\frac{3}{4}$ depth. Greenway[1989] analysed these measurements and showed that the logarithmic decrement of the first mode was independent of the total skip mass, but linearly dependent on rope length. The dimensionless damping ratio was of the order of 2.5%. The damping mechanism was not studied further, and proportional damping was assumed in the model. This resulted in strong attenuation of the higher modes. Mankowski [1986] experimentally examined the attenuation of kinetic shock waves travelling along the cable, and also the attenuation of the shock on entering the winder drum. The results of the study indicate that the winder drum may absorb as much as 66% of the energy of an incident kinetic shock. Mankowski notes that this result conflicts with that of Harvey[1965] who reported that " *Tests show that in a typical case, the amplitude of the disturbance is attenuated 0.65 % per 1000 meters of cable and by 1% at each pair of reflections at the drum and at the conveyance combined.*". One surmises that Harvey was referring to low frequency pulses with a large wave-length and longer periods than those applied in Mankowski's experiment, which were due to impact loading where the largest fundamental period of the applied pulse was 11ms. Harvey's results conform more readily with the logarithmic decrement associated with the first mode response, as measured during in-situ drop tests by Thomas et al.[1987].

Due to the potential complexity of the damping mechanism, this study follows the approach adopted by Greenway[1989], in that an equivalent viscous

damping coefficient is sought to model in some way the overall damping effect, without concern for the exact mechanism, which is likely to be highly complex and difficult to include in a simulation. The main concern however is the definition of a convenient and appropriate damping mechanism. Additional drop tests were performed at Elandsrand Gold Mine (Constancon[1992]). In these tests, a man cage was locked between the guides, loaded and suddenly released. The free response was monitored, and processed using standard parameter estimation routines. In order to investigate the higher longitudinal modes, electronic filtering was applied so as to amplify the response of the higher modes. The results of the parameter estimation confirmed that the dimensionless damping coefficient of the first mode was of the order of 3%, whilst the higher modes were were of a lesser value. The results of the drop test are presented in Appendix G. Greenway[1993] analysed these results and proposed a general proportional viscous damping mechanism, which reflects a lower damping effect in the higher modes. This damping mechanism is applied for convenience since an equivalent dimensionless modal damping coefficient can be calculated for each mode during the simulation.

5.6.2 Lateral Damping

Mankowski [1988] presented experimental measurements, defining a model of the lateral damping mechanism in terms of the time rate of change of curvature[14]. This model was considered by Mankowski on the basis that the inter-strand motion induced by an irrotational whirling action of the rope is proportional to the instantaneous curvature of the rope. Mankowski constructed an experimental facility to simulate irrotational whirling action of a typical mine rope. The experimental results presented indicate that the average power dissipation, and hence the equivalent viscous damping coefficients are low in comparison to the potential aerodynamic dissipation of the catenary. A detailed discussion regarding lateral dissipation is presented in Appendix H. Due to the lack of data concerning the lateral dissipation characteristics of mine hoist ropes, a proportional damping mechanism is assumed, where the value of $\zeta_1 = 0.05\%$ of critical damping is applied. This conforms to the order of dissipation determined in Mankowski's tests.

[14]The time rate of change of curvature results in a distributed damping force proportional to the stiffness properties of the rope.

5.7 Simulation of the Equations of Motion

The nonlinear ordinary differential equations of motion developed for the mine hoist system were simulated by applying the *Matlab-Simulink programme*. Simulink is a powerful simulation package based on the graphical definition of a block diagram description for the system equations. Having developed the block diagram for the system, pertinent physical data pertaining to the installation is supplied to the Simulink package via a *definition routine coded* and executed in the Matlab environment. A mask of input data required is tabulated in table 5.1.

Since the system characteristics change with time, and consequently depth during the simulation, a look-up table is applied to define the relationship between the angular winding velocity and depth. Additional look-up tables define the longitudinal and lateral natural frequencies, as well as the variation in the longitudinal damping coefficients, and the Lebus drum excitation and layer change excitation as a function of depth. These tables are defined prior to the simulation, and are interpolated during the simulation. This format *efficiently accounts* for the time dependence of the system parameters during the simulation.

Simulink provides a choice as to the type of integration routine applied. An automatic *step size Adams-Gear* routine was applied, with a relative error tolerance of 10^{-6}, and a maximum step size of 10^{-3} seconds. The maximum step size tolerance is specified to ensure sufficient accuracy with regard to the excitation look up tables.

In the normal mode simulation introduced in section 5.2, the excitation at the winder drum was accounted for by considering the first two harmonics of the Lebus groove profile, as presented in Appendix A. To better emulate the impulsive nature of the excitation, *a look-up table* was defined to accurately model the longitudinal and lateral excitation at the drum, as a function of shaft depth. Mankowski approximated the three dimensional displacement imparted to the rope at a coil cross-over as versine functions. This definition is applied, where the periodic displacement in the u, v, w *direction at the drum is defined* as a function of drum rotation. It is possible to define these displacement functions as a function of shaft depth, and hence drum rotation via a look-up table for the entire winding cycle. Since the lateral excitation is introduced via the lateral acceleration of the the cable, *it is a simple manner to construct* the appropriate look-up table by differentiating the lateral displacement profile analytically. The lateral excitation induced at a layer change is applied in a similar fashion. The definition of the Lebus coil cross-over excitation, as well

as the layer change excitation is presented in Appendix A.

The periodic longitudinal excitation due to the coil cross-over profile is introduced to the system by $F_g(t)$. The definition of $F_g(t)$ requires that the periodic axial displacement at the drum $u(0,t)$ as well as the gross lateral motion across the drum surface is accounted for. The longitudinal excitation due to a layer change is introduced by adding an additional longitudinal displacement to the periodic axial displacement at the layer change, and holding this value constant until it increases at the next layer change. The direction of the wind influences the longitudinal excitation definition, in that during an ascending wind the periodic pulses due to the coiling profile, and transient pulses induced at a layer change are tensile, whilst during the descending wind they are compressive.

Table 5.1: Simulation variables

N-lat	Number of in and out of plane lateral modes.
N-Long	Number of longitudinal modes.
J	Sheave Inertia.
M	Skip Mass.
M0	Skip Pay-load.
m	Linear Rope density.
a	Acceleration/Deceleration.
V	Nominal Winding Speed.
De	Depth of wind.
Lc	Catenary Length.
E	Effective Youngs Modulus of the rope.
Ax	Effective steel area of the rope.
β	Cross over arc.
Dd	Drum Diameter.
Ds	Sheave Diameter.
Dr	Rope Diameter.
Lx	Layer cross over points.
μ_a, μ_b	Longitudinal proportional material damping factors.
ζ^{lat}	Lateral proportional modal damping factor of the first mode.

5.8 Kloof Mine Simulation

A simulation of the ascending and descending winding cycle on the Kloof mine was conducted. The purpose of the simulation was to assess the degree of correlation achievable via a comparison of the the qualitative observations presented by Dimitriou and Whillier[1973].

The parameters applied in the simulation are presented in table 5.2.

Table 5.2: Simulation variables - Kloof Mine

$N-lat$	Number of in and out-of-plane lateral modes.	4
N-Long	Number of longitudinal modes.	4
J	Sheave Inertia.	15200 kgm^2
M	Skip Mass.	7920 kg
M0	Skip Pay-load.	9664 kg
m	Linear Rope density.	8.4 kg/m
a	Acceleration/Deceleration.	$0.74m/s^2$
V	Nominal Winding Speed.	15 m/s
De	Depth of wind.	2100m
Lc	Catenary Length.	74.95 m
E	Effective Youngs Modulus of the rope.	$1.1 \times 10^{11} N/m^2$
Ax	Effective steel area of the rope.	$0.001028m^2$
β	Cross over arc.	0.2 rad
Dd	Drum Diameter.	4.28 m
Ds	Sheave Diameter.	4.26 m
Dr	Rope Diameter.	0.048 m
Lx	Layer cross over points.	525m, 1050m, 1575m
μ_a	General proportional damping parameter	0.159
$\mu_b(s_2)$	General proportional damping parameter	$10.49s_2$
ζ_1^{lat}	Lateral proportional modal damping ratio	0.05%

Since the physical parameters of a realistic system are difficult to quantify accurately, and may change during the life of the rope [15], a sensitivity analysis was conducted with respect to the nominal winding speed. In this study,

[15]For instance, the payload mass may vary by 5% from cycle to cycle. Manufacturing tolerances will result in variations in the nominal rope properties. The manufacturers tolerance on the linear mass density is -7%-0%, and -1%-4% on the rope diameter (Haggie Rand [1990]).The layer change locations vary during the life of the rope, since control of rope deterioration at layer and turn cross-overs requires that the *back end* (ie. drum end) be pulled in at short intervals of about six weeks. The front end of the rope is cut and

the winding speed was changed incrementally from 14 m/s to 16 m/s in 0.2 m/s increments, for both the ascending and descending cycle. The results of the sensitivity study are presented in Appendix L. The sensitivity study indicated that the response is sensitive to the winding velocity, in that the amplitude of a resonant condition is sensitive to the layer change location with respect to the resonant condition. On the basis of the sensitivity study, a winding velocity of 14.8 m/s was selected as being representative of the winder condition, since severe dynamic motion occurred on the ascending cycle. This winding condition was judged to be sufficiently close to that considered by Dimitriou and Whillier[1973], and Mankowski[1982], to be representative of the Kloof Mine hoist winder.

The results from the simulation are presented in figures 5.9 -5.12 for the descending cycle, and 5.15 -5.19 for the ascending cycle. Each simulation consists of:

- The lateral in-plane response at the first quarter point of the rope vs. shaft depth.
- The lateral out-of-plane response at the first quarter point of the rope vs. shaft depth.
- The longitudinal elastic response at the sheave vs. shaft depth.
- The longitudinal elastic response at the skip vs. shaft depth.
- The total rope tension on the catenary side of the sheave vs. shaft depth.
- The total rope tension on the shaft side of the sheave vs. shaft depth.
- The rope tension ratio across the sheave vs. shaft depth.
- The lateral in-plane modal amplitudes vs. shaft depth.
- The lateral out-of-plane modal amplitudes vs. shaft depth.

All figures are headed by a linear frequency map of the system. This map illustrates the relationship between the first two harmonics of the Lebus groove excitation frequency, the first four longitudinal and lateral natural frequencies, and the layer change location. The Lebus groove excitation frequency is

tested every six months in accordance with statutory requirements. The ammount cut off the front end, and the ammount of rope lost due to pulling is augmented by using up spare *dead* turns on the drum. A minimum of three *dead* turns is always required on the drum, but additional dead turns are allowed for compensation purposes.

represented by dashed lines; the longitudinal frequencies by dotted lines, and the lateral natural frequencies by solid lines. The layer change locations are represented by vertical lines.

The figures relating to the in-plane lateral motion at the first quarter point of the catenary, are constructed to reflect both the dynamic amplitudes, and the change in rope curvature with depth. This is achieved by referencing the motion to the span line between the end points of the catenary. As the vertical rope length changes, the equilibrium curvature of the cable changes, and hence the mean static position of the cable changes. Thus the in-plane displacement is calculated as[16]:

$$v(\frac{l_c}{4},t) = -\frac{3}{32}\kappa l_c^2 + \sum_{i=1}^{4} \sin(\frac{i\pi}{4}) q_i(t)$$

The tension ratio across the sheave is presented to ascertain if rope slip occurs during the simulation. A simple bollard type friction analysis as presented by Mankowski[1982] indicates that if the tension ratio lies beyond the limits of $0.625 \rightarrow 1.60$ then slip will occur. Since the possibility of slip is not accounted for in the simulation, this condition would invalidate the simulation beyond that time.

The results presented in figures 5.9 -5.12 for the descending cycle should be read from left to right, whilst those presented in figures 5.15 -5.19 for the ascending cycle should be read from right to left.

[16]The equilibrium profile of the rope, measured from the span line is: $Z = \frac{X}{2}(1-X)$, where $Z = -\frac{Hz}{mgl_c^2}$ and $X = \frac{x}{l_c}$, thus $z(\frac{l_c}{4}) = -\frac{3mgl_c^2}{32H}$, and $\kappa = \frac{mg}{H}$, hence $z(\frac{l_c}{4}) = -\frac{3\kappa l_c^2}{32}$

5.9 Simulation Results

5.9.1 Descending Cycle

The simulation results for the descending cycle are presented graphically in figures 5.9-5.14. General observations concerning the simulation of the descending cycle are:

- When the skip accelerates down the shaft, the average rope tension in the catenary drops, and consequently the in-plane motion is off-set in the negative direction. This effect is observed in the odd in-plane modes which are capable of geometric adjustment to account for the change in tension. The reverse effect is noted when the skip is decelerated to rest at the end of the wind.
- The layer change over is evident in the the in-plane lateral response, where it induces transient motion.
- The nonlinear interaction between the lateral and longitudinal modes is evident, where an increase in the catenary motion causes a negative drift in the longitudinal motion at the sheave.
- The motion at the sheave drifts in accordance with the gross lateral motion across the drum. Thus a triangular wave form is perceptible, where the motion drifts in the negative direction between the start of the wind and the first layer change, drifting in the opposite direction during the second layer; this effect repeats itself, and reflects the increase in the rope length due to rope traversing between the drum cheeks.

Specific observations regarding the descending cycle are:

- The in-plane motion remains small through-out the wind.
- The tension ratio across the sheave remains within the no-slip region, and thus slip across the sheave does not occur.
- The out-of-plane motion grows towards the end of the cycle. This occurs since the even (second and fourth etc) catenary modes approach a resonant condition with the Lebus excitation frequency at approximately 1900m.

- At approximately 1700m, the second catenary mode and the third longitudinal mode are equal, promoting coupling between the longitudinal and lateral motion. In effect a condition of combination resonance may occur, where the second lateral and third longitudinal modes are equal to the second Lebus excitation frequency (refer to the stationary stability plot presented in figure 4.7).

- The deceleration cycle begins at approximately 1950 m, and longitudinal transients occur.

- The attenuation of the dynamic tension across the sheave, illustrates a significant filtering action, which tends to isolate the catenary from the vertical section.

The sensitivity of the system to the winding speed is well illustrated by considering the resonant condition towards the end of the wind. Figures 5.13,5.14 present results from the sensitivity study for a winding velocity of 14.6 and 15 m/s respectively. Whilst the lateral out-of-plane motion reduces at a winding velocity of 15 m/s since the passage through resonance is not completed prior to the deceleration cycle, very different conclusions regarding the dynamic integrity of the system would be drawn from the simulation results at 14.6 m/s. In the latter condition of tuning, the resonant condition occurs at approximately 1700m; sufficient time exists for the out-of-plane motion to grow sufficiently to induce in-plane motion, and consequently significant tension fluctuations occur in the catenary from 1600m onwards. Since the lateral frequency lines have a low slope, relatively small changes in the winding speed result in significant shifts in the resonant conditions, and consequently different behaviour.

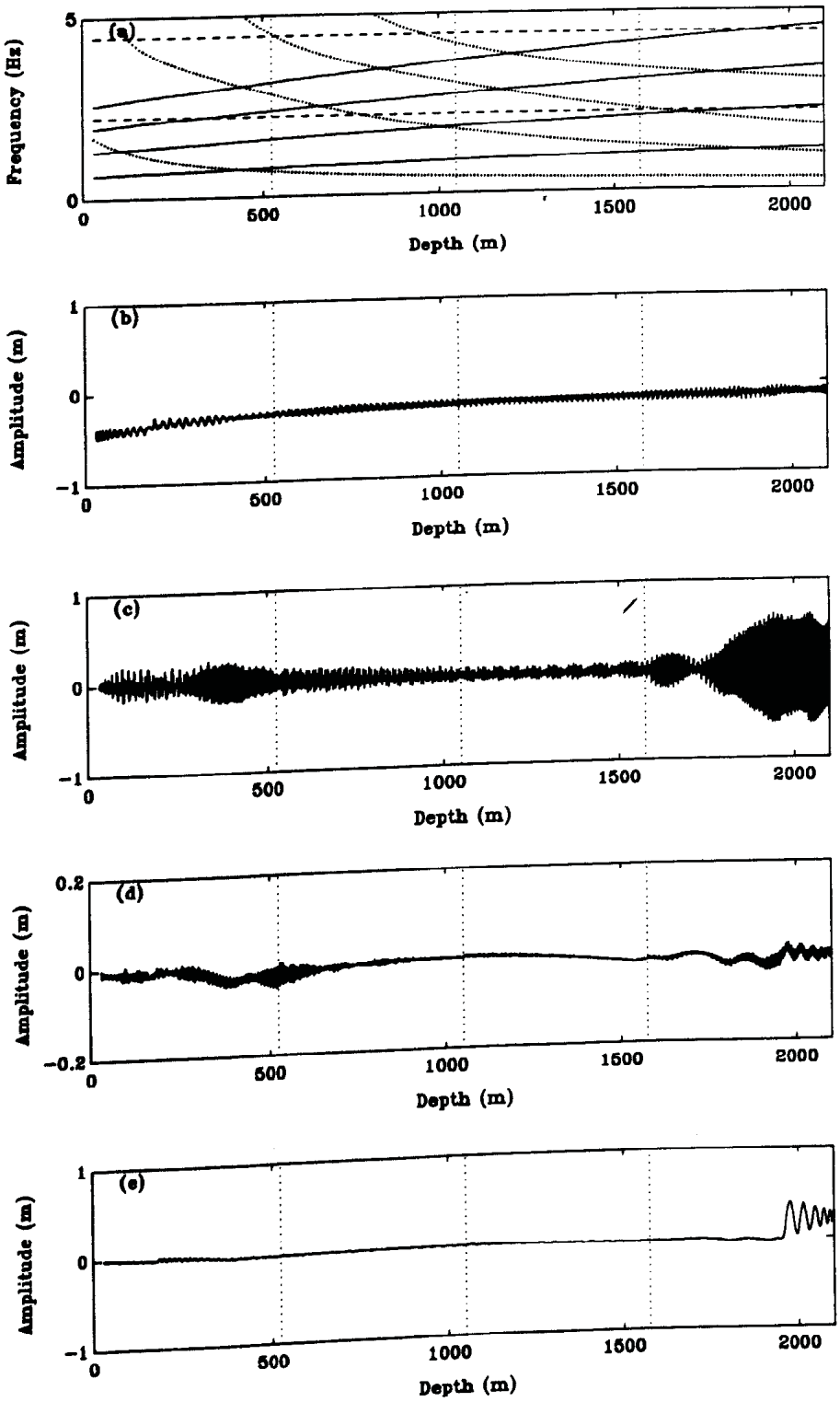

Figure 5.9: Descending cycle: Kloof Mine hoist system: 14.8 m/s

a) Linear Frequency Map
b) In-Plane Response $s = l_c/4$
c) Out-of-Plane Response $s = l_c/4$
d) Sheave Response
e) Skip Response

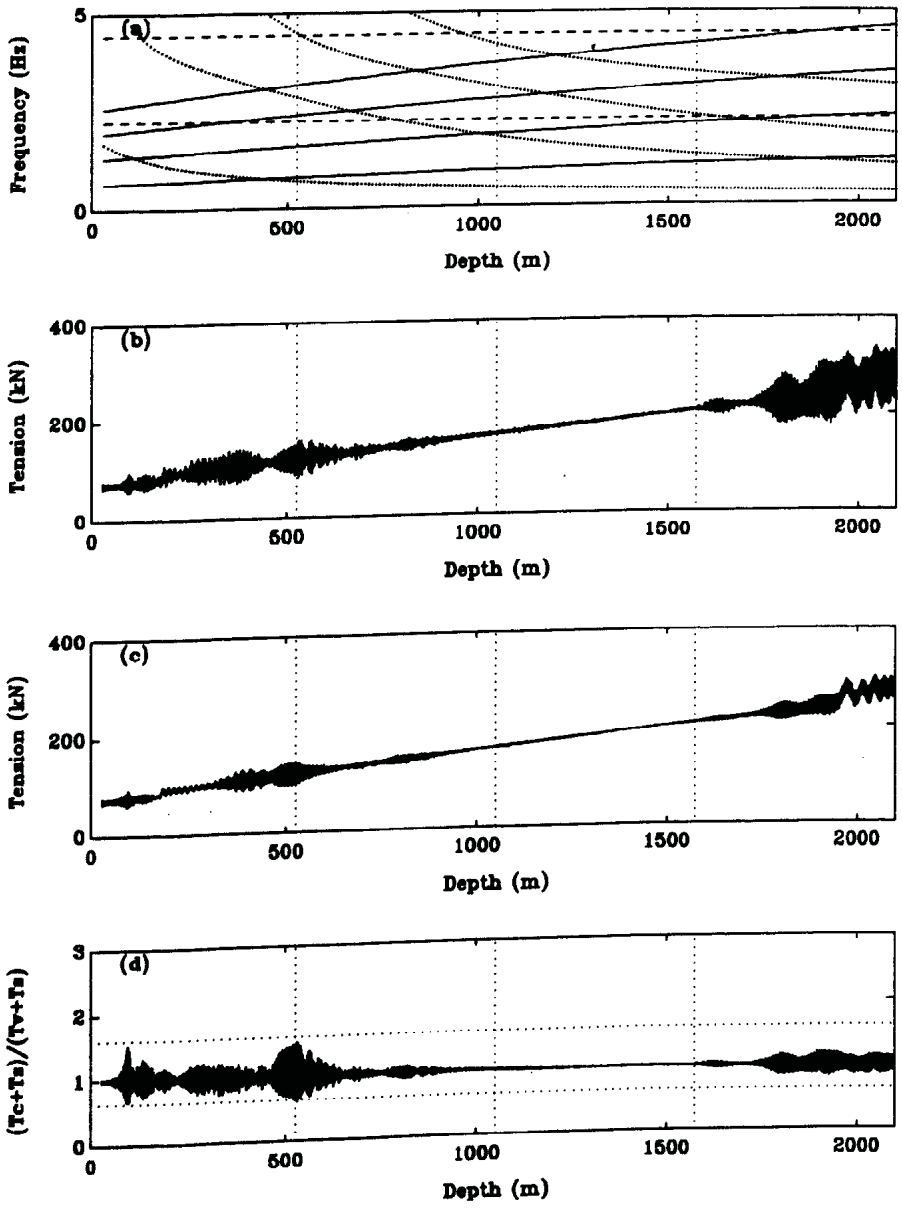

Figure 5.10: Descending cycle: Kloof Mine hoist system: 14.8 m/s

a) Linear Frequency Map
b) Total Catenary Tension
c) Total Vertical Rope Tension $s = l_c$
d) Tension Ratio Across the Sheave $R = \frac{T_c+T_s}{T_v+T_s}$

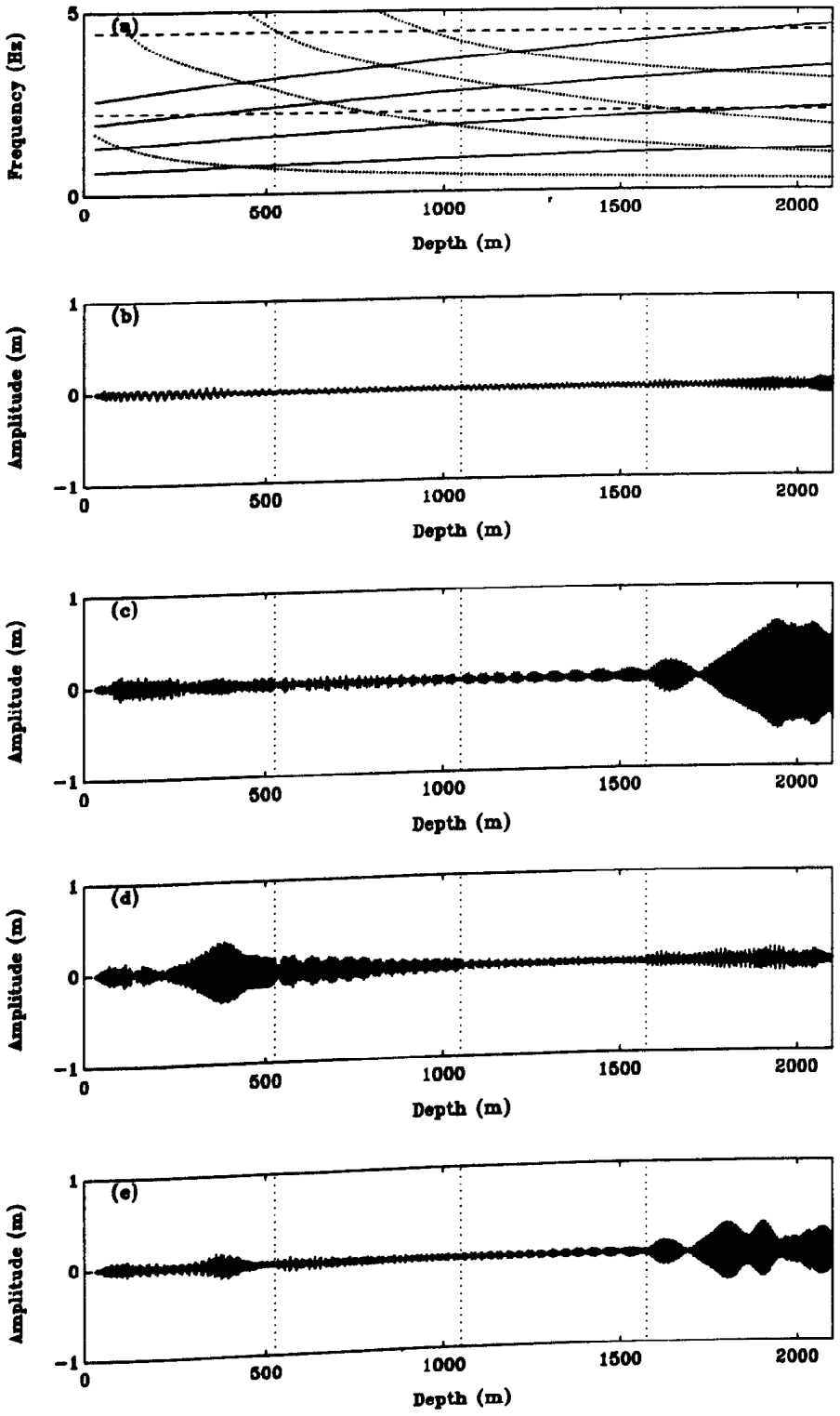

Figure 5.11: Descending cycle: Out-of-plane modal amplitudes: 14.8 m/s

a) Linear Frequency Map, b) $q_1(t)$, c) $q_2(t)$, d) $q_3(t)$, e) $q_4(t)$

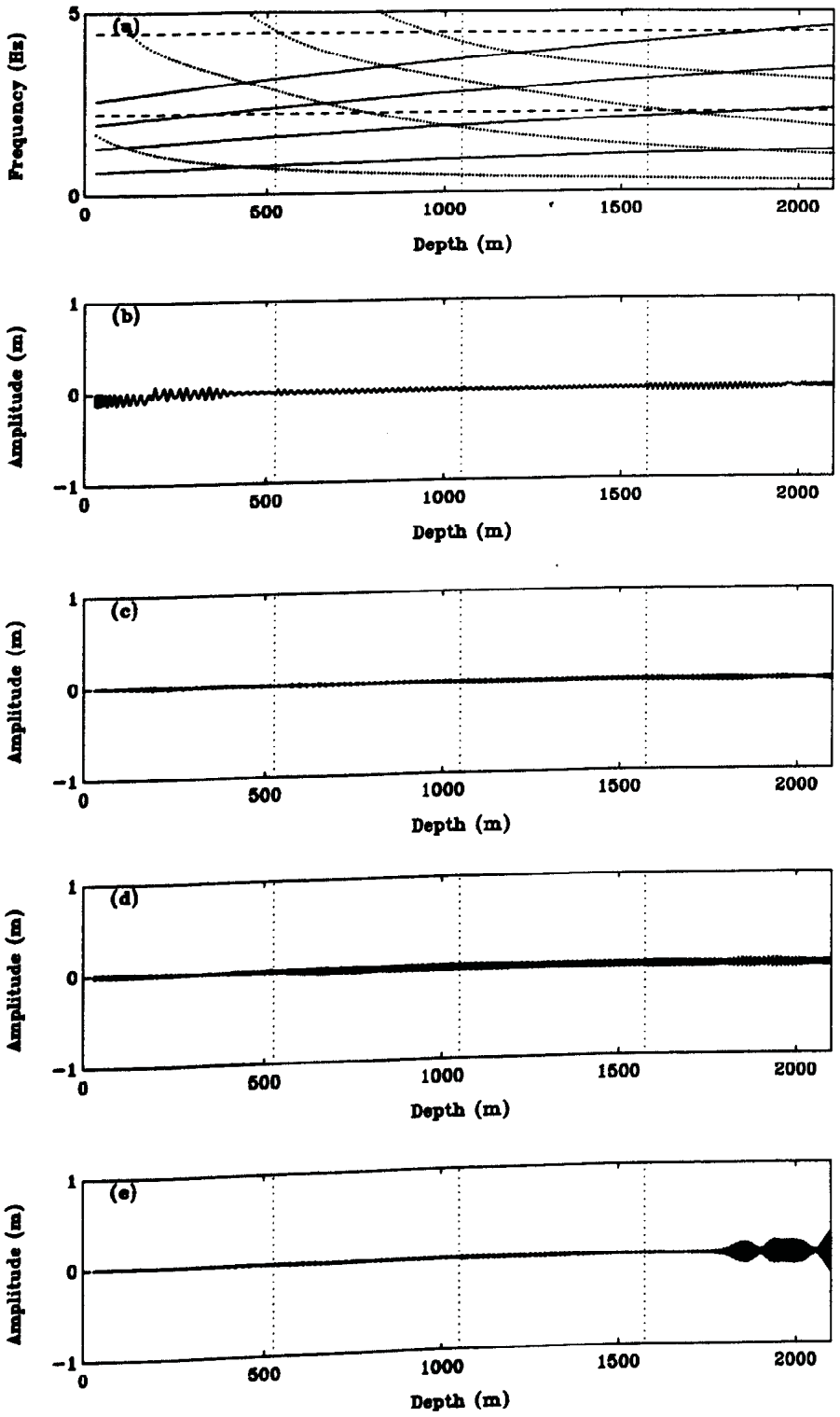

Figure 5.12: Descending cycle: In-plane modal amplitudes: 14.8 m/s

a) Linear Frequency Map, b) $r_1(t)$, c) $r_2(t)$, d) $r_3(t)$, e) $r_4(t)$

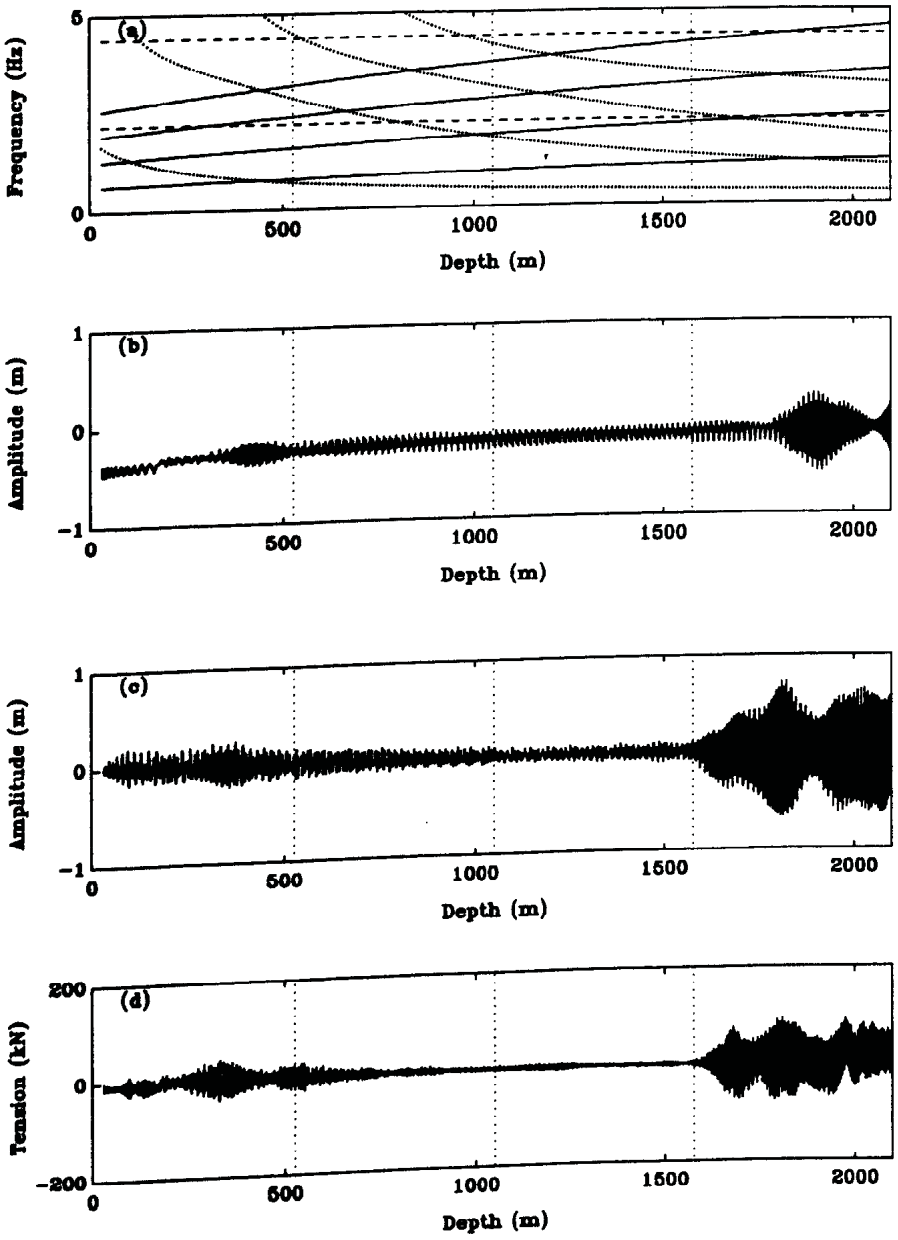

Figure 5.13: Descending cycle: Kloof Mine hoist system: 14.6 m/s
a) Linear Frequency Map.
b) In-Plane Motion - $s = l_c/4$.
c) Out-of-Plane Motion - $s = l_c/4$.
d) Dynamic Catenary Tension.

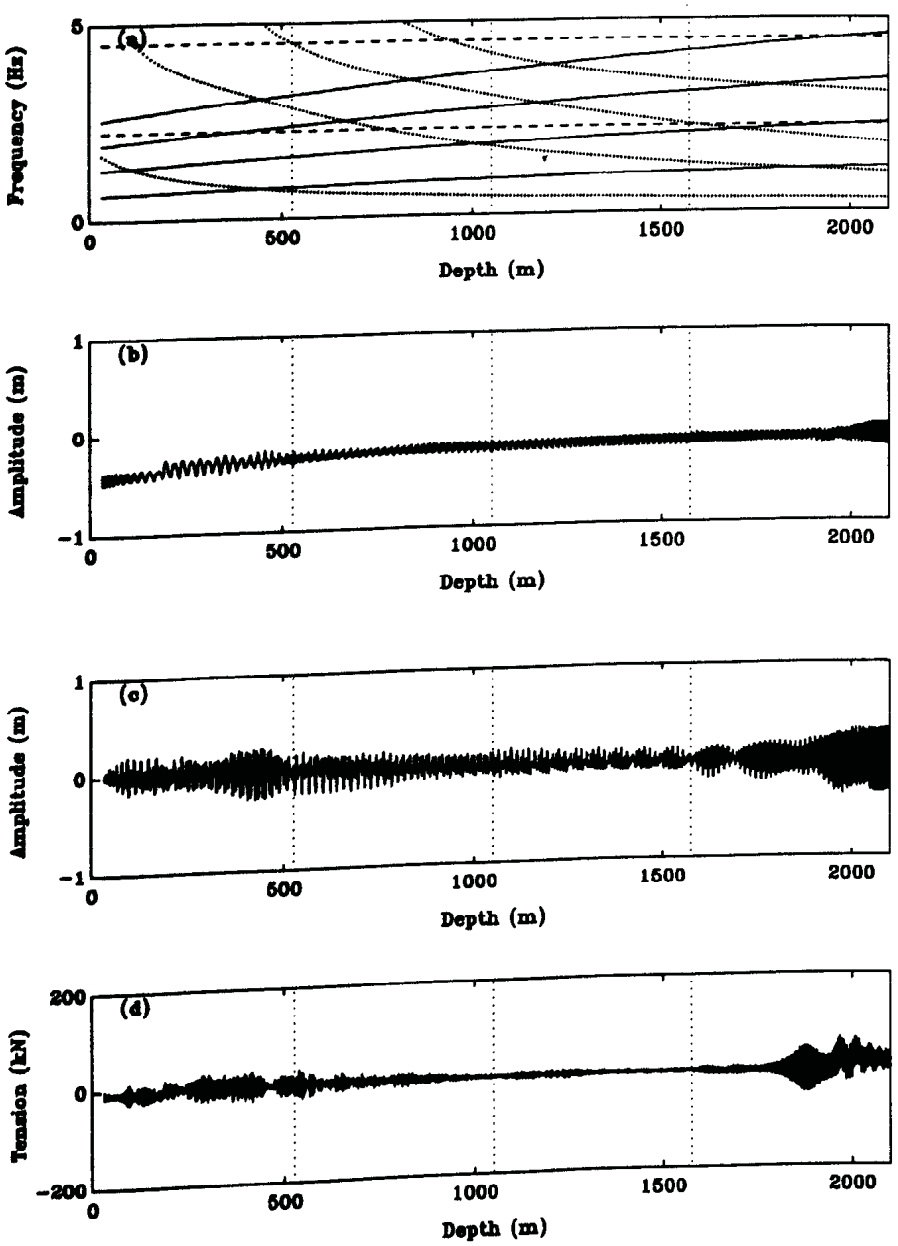

Figure 5.14: Descending cycle: Kloof Mine hoist system: 15 m/s
a) Linear Frequency Map.
b) In-Plane Motion - $s = l_c/4$.
c) Out-of-Plane Motion - $s = l_c/4$.
d) Dynamic Catenary Tension.

5.9.2 Ascending Cycle

The simulated response of the ascending cycle is presented in figures (5.15-5.23). This simulation predicts significant dynamic response, where rope whip occurs and lateral amplitudes of the order of 1m arise in the catenary section. The tension ratio across the sheave exceeds the limits for no slip at approximately 300m, and consequently the simulation would not be realistic above this depth. The rapid growth in the second in-plane mode, reflected in figure 5.18(c), prior to this condition presents convincing evidence of problematic dynamic behaviour. It is noted that according to the stationary linear frequency map, the system is tuned such that the second and fourth out-of-plane modes are directly excited in resonance at approximately 700m. The peak response in the directly excited second and fourth lateral out-of-plane modes occurs in this vicinity. The in-plane response increases after the out-of-plane response has grown. Since the in-plane response is lightly excited, this response is mainly associated with the nonlinear coupling between the in and out-of-plane modes, which is consistent with the autoparametric nature of the system, whereby out-of-plane motion couples to parametrically excite in-plane motion. During the ascending cycle, the Lebus excitation frequency is constant, whilst the lateral natural frequencies reduce with depth. Thus the passage through resonance occurs with the excitation frequency passing from below to above the natural frequency. This is similar to the laboratory model with a positive sweep rate, where as the excitation frequency increased, the lateral out-of-plane motion increased, followed by a bifurcation of the trivial in-plane motion. A plateau region subsequently occurred, where the lateral motion became saturated and significant longitudinal dynamic motion occurred. This behaviour is reflected in the simulation, where the amplitude envelope of the modal response of the even in and out-of-plane lateral modes reflects such a pattern (refer to figures 5.17, 5.18).

The polar response of the catenary is illustrated at four different depths in figures (5.19-5.23); at the start of the wind the motion is essentially planar, becoming almost circular in shape between the depth of 700-500 m. Thereafter, the circular motion gives way to an elliptic orbit, and consequently large fluctuations in the catenary tension arise. It is assumed that the latter region would be termed rope whip by Dimitriou and Whillier[1973]. According to the numerical simulation, the whip is so severe that a slack rope condition is approached during the orbit, which clearly represents very severe dynamic behaviour.

On assessing the overall dynamic response, the auto-parametric nature of the system is evident. An autoparametric mechanism arises when the motion in

a directly excited mode provides parametric excitation leading to response in modes which are not directly excited. This effect is important when conditions of internal resonance exist in the system, as such a condition promotes intermodal response. This situation has been discussed in the literature (Ashworth and Barr[1987], Bux and Roberts[1986],Cartmell and Roberts[1988]), where cascading modal interactions arise, and the directly excited response parametrically excites another mode, which in turn excites a further mode, and so on. Such behaviour occurs with regard to the out-of-plane and in-plane motion, where out-of-plane response parametrically excites in-plane motion. It was expected that the longitudinal system would promote further intermodal response. However, since the sheave tends to isolate the catenary from the vertical system due to its large inertia, such regions of secondary resonance are not clearly evident in the simulated response. It is important to note that in-plane amplitudes of the order of 1m arise, where the direct in-plane excitation is of the order of 0.5 mm. This emphasises the difference between a linear analysis, where in-plane motion would arise purely due to the direct excitation; clearly this amplitude occurs as a result of the nonlinear coupling inherent in the system.

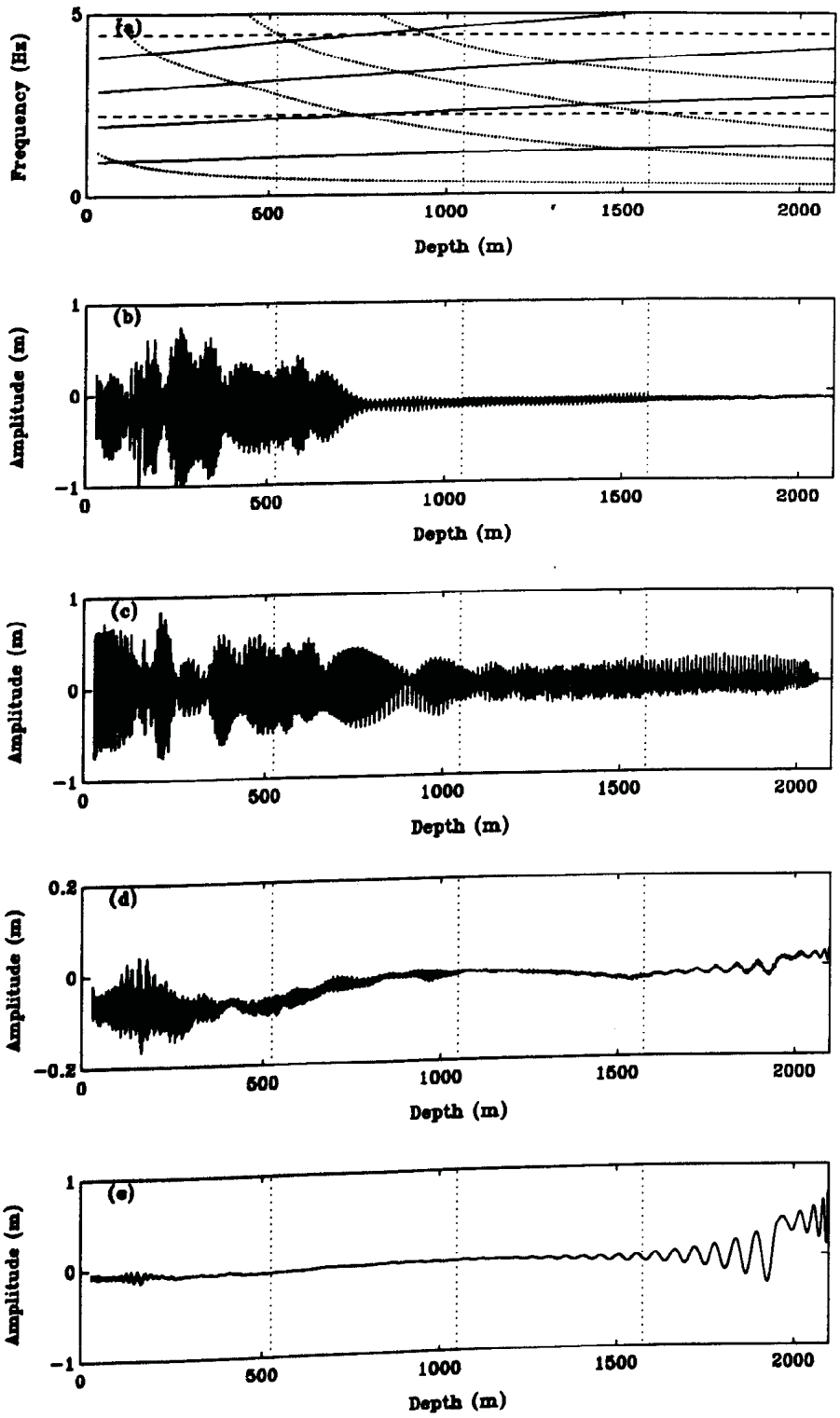

Figure 5.15: Ascending cycle: Kloof Mine hoist system: 14.8 m/s

a) Linear Frequency Map
b) In-Plane Response $s = l_c/4$
c) Out-of-Plane Response $s = l_c/4$
d) Sheave Response
e) Skip Response

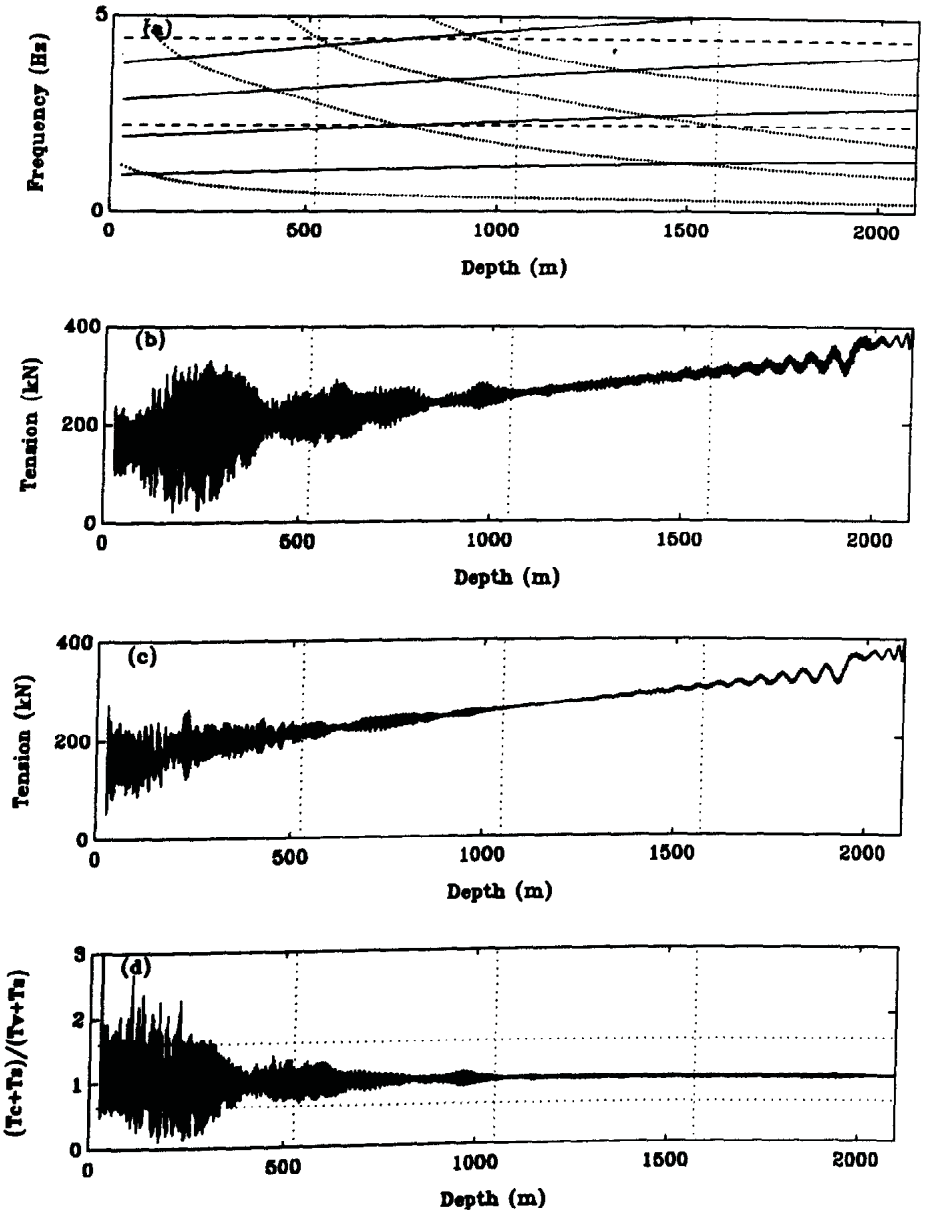

Figure 5.16: Ascending cycle: Kloof Mine hoist system: 14.8 m/s

a) Linear Frequency Map

b) Total Catenary Tension

c) Total Vertical Rope Tension $s = l_c$

d) Tension Ratio Across the Sheave $R = \frac{T_c+T_s}{T_v+T_s}$

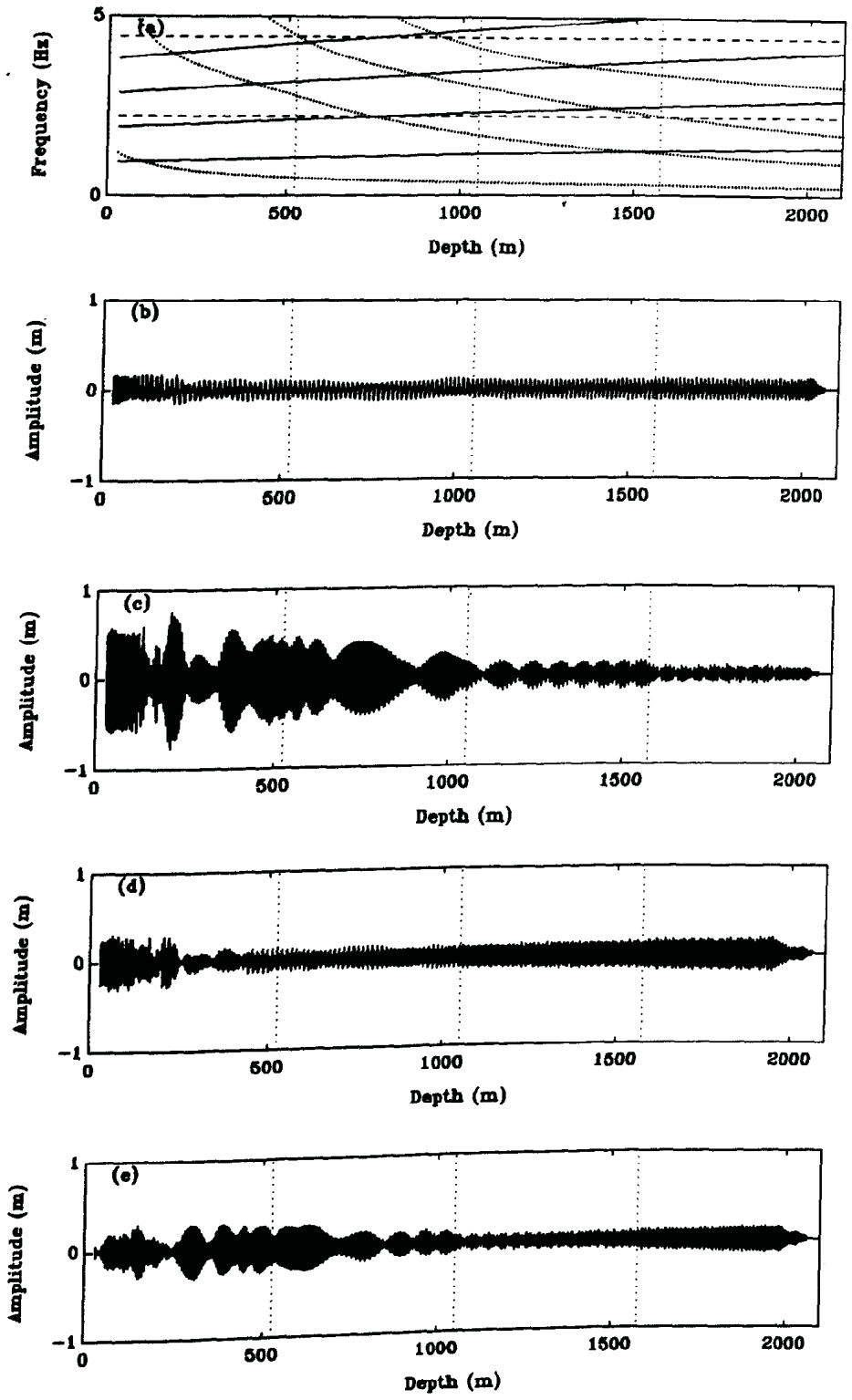

Figure 5.17: Ascending cycle: Out-of-plane modal amplitudes: 14.8 m/s

a) Linear Frequency Map, b) $q_1(t)$, c) $q_2(t)$, d) $q_3(t)$, e) $q_4(t)$

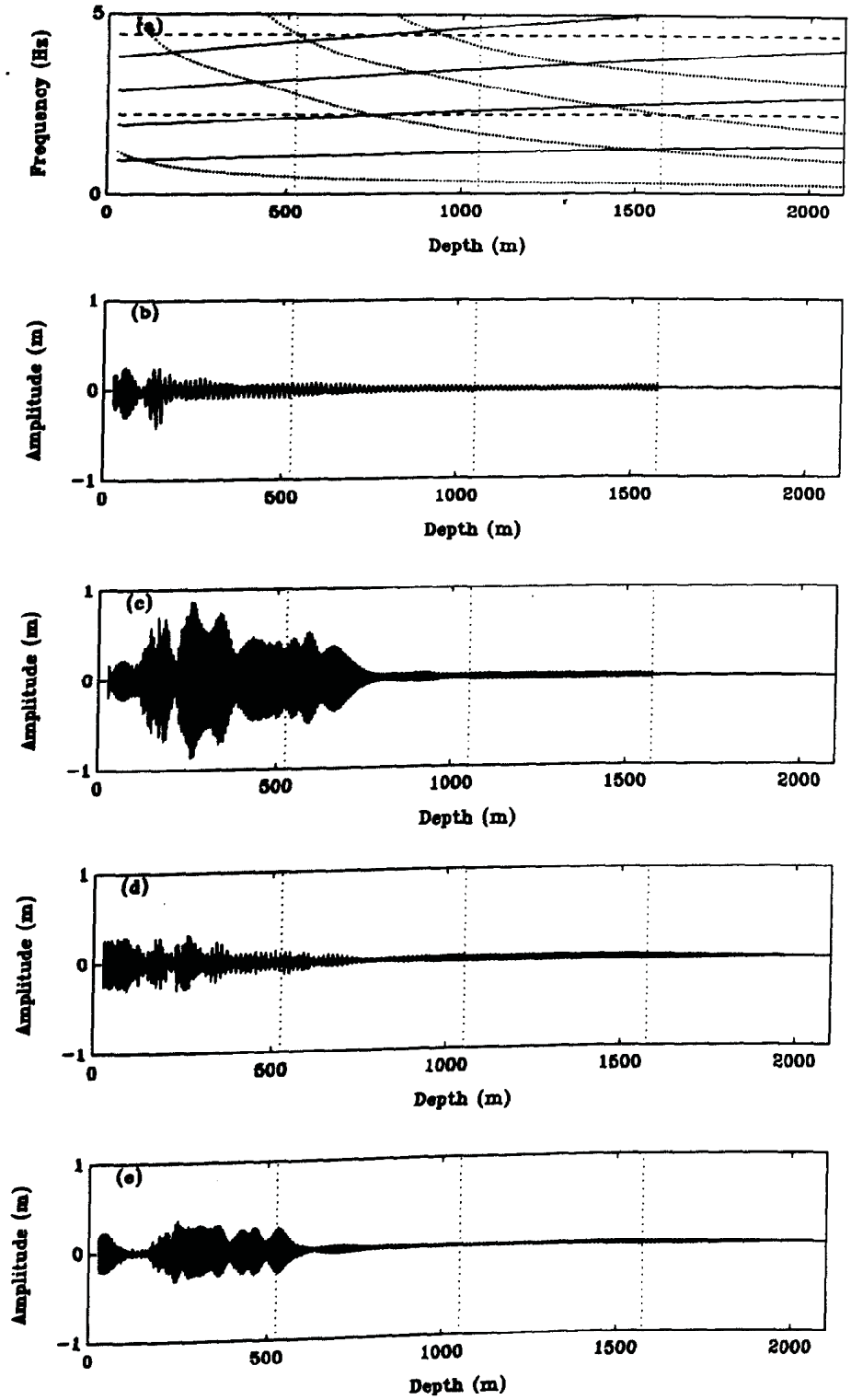

Figure 5.18: Ascending cycle: In-plane modal amplitudes: 14.8 m/s

a) Linear Frequency Map, b) $r_1(t)$, c) $r_2(t)$, d) $r_3(t)$, e) $r_4(t)$

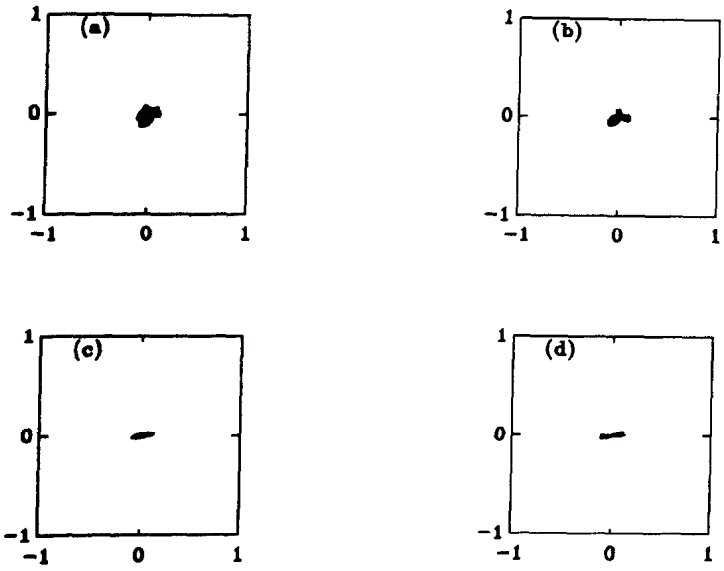

Figure 5.19: Ascending cycle: First mode polar plot
First Mode Polar Plot, Amplitude (m).
a) Depth 300-400 m. b) Depth 500-700 m.
c) Depth 900-1000 m. d) Depth 1500-1600 m.

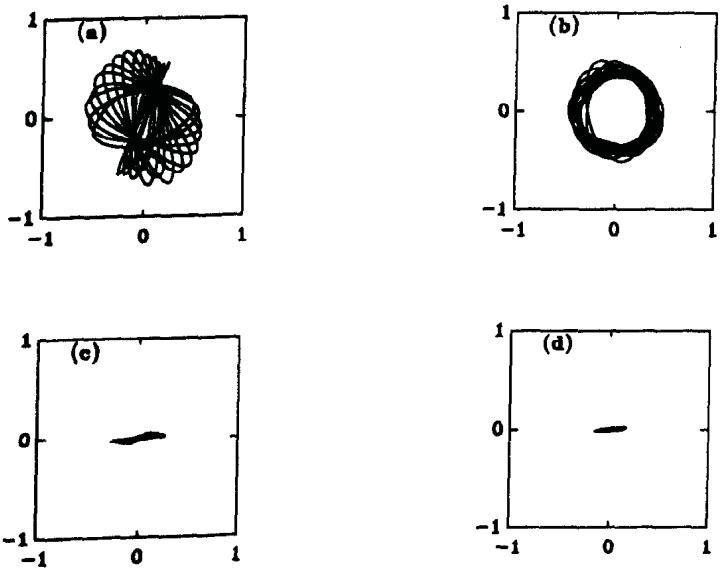

Figure 5.20: Ascending cycle: Second mode polar plot
Second Mode Polar Plot, Amplitude (m).
a) Depth 300-400 m. b) Depth 500-700 m.
c) Depth 900-1000 m. d) Depth 1500-1600 m.

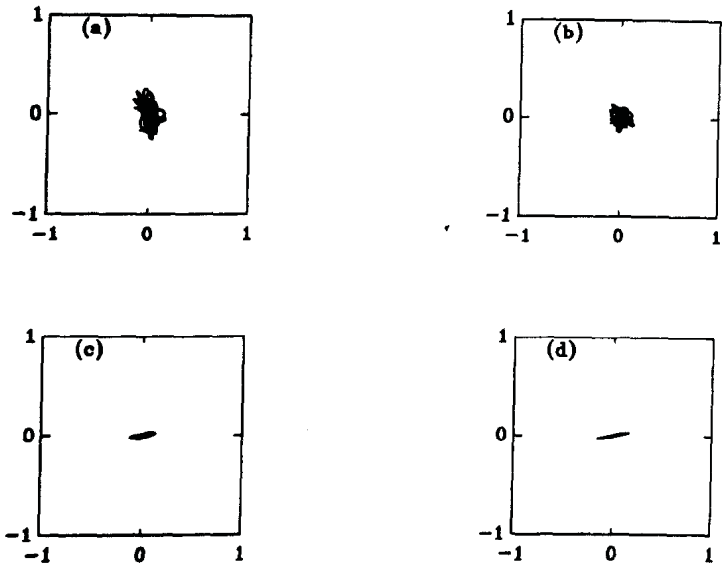

Figure 5.21: Ascending cycle: Third mode polar plot
Third Mode Polar Plot, Amplitude (m).
a) Depth 300-400 m. b) Depth 500-700 m.
c) Depth 900-1000 m. d) Depth 1500-1600 m.

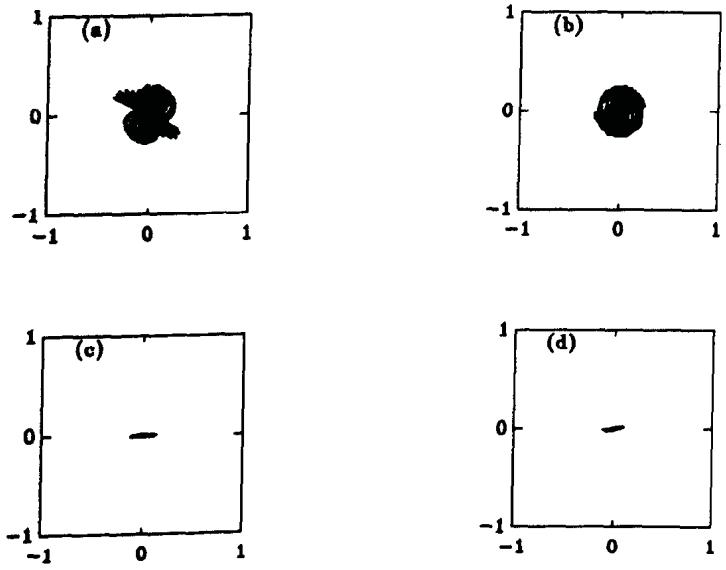

Figure 5.22: Ascending cycle: Fourth mode polar plot
Fourth Mode Polar Plot, Amplitude (m).
a) Depth 300-400 m. b) Depth 500-700 m.
c) Depth 900-1000 m. d) Depth 1500-1600 m.

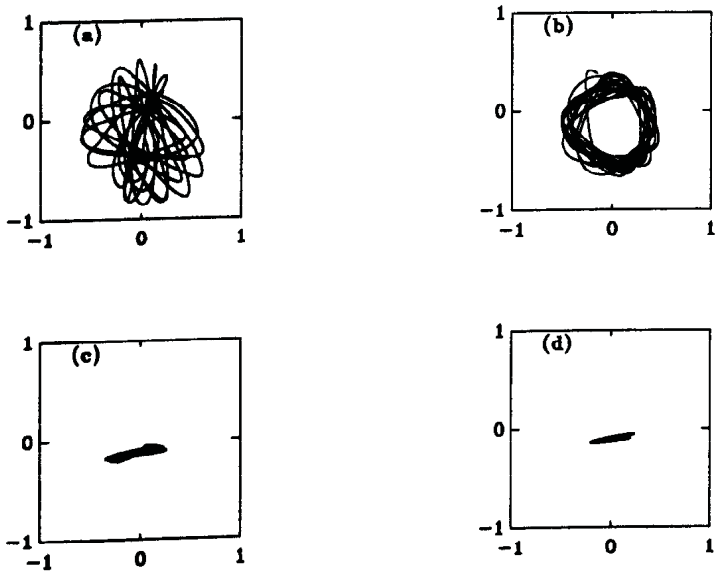

Figure 5.23: Ascending cycle: Polar plot of the response, $s = l_c/4$
Total Response Polar Plot, $s = l_c/4$, Amplitude (m).
a) Depth 300-400 m. b) Depth 500-700 m.
c) Depth 900-1000 m. d) Depth 1500-1600 m.

5.9.3 Dimitriou and Whillier's Observations

Dimitriou and Whillier[1973] considered the Kloof Mine hoist system, and documented observations regarding the motion. These observations are extracted and presented below.

Visual accounts of the dynamic behaviour of the catenaries at Kloof have been recorded over more than a three year period. Some variations have occurred during that time but regular features have been noted and these are numbered below for easy reference. The period of main interest covers the second half of the hoisting cycle, when a full skip is raised, and consists of two distinct phases, marked in figure 1.5.

Phase 1 starts at approximately t=110 s, when the skip is about 900 m below the headsheave, and lasts for about 20 s.

Phase 2 starts at the cross-over from the third to the fourth cable layer on the drum and ends when the skip is at the top of the wind.

Feature 1: All catenaries vibrate to some extent during most of the hoisting cycle, both during raising and lowering of the skips. Except during phases 1 and 2, these vibrations have no clearly defined mode and have small amplitudes. The amplitudes are smaller and the frequencies are higher when the skip is near the bottom of the shaft.

Feature 2: During phase 1, the amplitudes increase and the catenaries settle into a clearly defined second mode for the horizontal and vertical transverse components. The amplitude of the horizontal component is usually larger. Cables A and D[17], in that order, have the greatest amplitude, which is judged to be of the order of 1 m. On occasions, these vibrations continue throughout phase 2 with a gradual change in mode but no perceptible change in amplitude. On other occasions the mode of vibration loses its clear definition at the beginning of phase 2 and the amplitude decreases.

Feature 3: During phase 1 the vertical cables start vibrating transversely. The amplitude, viewed at the collar of the shaft, increases in about 15 s to a maximum of approximately 0.1 m. These vibrations continue, at maximum amplitude throughout phase 2. The vibrations are too rapid for the frequency to be judged by eye. However, a photograph of the vertical cables exhibits an approximate half sine wave of about 40 m length. This indicates that the main wavelength is the same as for the catenaries and the main frequency is ap-

[17]Cables A-D are defined in çhapter 1, section 1.2.2.

proximately 2 Hz (but superimposed harmonics give the appearance of a higher frequency to the naked eye.).

Feature 4: On occasions, at the beginning of phase 2, the vibrations of cable A develop a vertical component with an amplitude in excess of 2 m. The cable appears to come down with the speed of a whip. Whenever this occurs the speed of winding is reduced by the operator and this behaviour has not been subjected to regular observation. One observer believes he saw a first mode pattern in the large vertical component of the whip, but this observation has not been corroborated.

Feature 5: None of features 2,3 and 4, is in evidence when the skips are lowered. In particular the vertical cables do not vibrate.

Feature 6: Every six weeks a length of cable is cut at the compensating sheave and the dead coils are pulled over the drum to change the position of the cross-overs. Immediately after this, the vibrations during phases 1 and 2 have their maximum amplitude. The amplitude decreases gradually during the six week interval and the plant can usually be run at full winding speed during the second half of the interval.

Feature 7: An experiment had been tried by the engineering staff at Kloof: the speed of winding was decreased abruptly at the beginning of phase 1. It was found that a drop in speed in this manner from 15 to 14 m/s was sufficient to reduce considerably the amplitude of the vibrations during the remainder of phases 1 and 2.

The simulated behaviour presented in this study largely confirms these observations. The only notable difference is the lack of reported dynamic motion on the descending cycle. It is important to realise that Dimitriou and Whillier's observations were visual, and perhaps they were more sensitive to observations regarding in-plane motion. The lack of in-plane motion in the descending simulation therefor correlates with these observations. Furthermore, the sensitivity of the system to the winding speed is an important consideration. In this regard an increase in winding speed to 14.9 m/s would place this region within the decelerating region, where transverse motion would be viewed as normal. Unfortunately the winder on this system was changed in the late 70's, and further experimental results could not be extracted.

5.10 Conclusion

The simulation exercise conducted has been successful in describing adverse dynamic behaviour at the Kloof mine. It is noted however, that this is a numerical simulation and consequently is constrained by necessary assumptions, for instance the assumption of a proportional lateral and longitudinal damping mechanism, and the neglect of the lateral motion of the vertical rope. It is also important to note that the winder is treated as an ideal energy source, and that no account was made for the flexibility of the headgear structure. Thus any claim that the simulation approaches a precise description of the actual motion would be dubious. Nevertheless, since the equations of motion developed describe the physical nature of the system, it is expected that adverse dynamic behaviour in the simulation would support the notion of adverse dynamic behaviour in reality, and draw attention to this condition of tuning during a design exercise. Thus good engineering judgement would be required to interpret the simulation results.

The assumption in industry that the catenary motion does not generate significant tension fluctuations, and hence any assumption that adverse dynamic catenary motion has no bearing on the fatigue life of the rope is clearly questionable. Significant tension fluctuations were observed in the catenary during the simulated ascending cycle. Although these may be tempered in reality by the support structure flexibility, adverse dynamic catenary motion will result in significant tension fluctuations.

A number of features have been observed during the simulation exercise, which may be used to advantage to improve the dynamic integrity of an existing installation, without changing the geometric parameters of the system. These are itemised below:

- The periodic axial and lateral excitation due to the Lebus cross-over can be reduced, and hence the possibility for whip reduced, by increasing the cross-over arc length, and by profiling the grooves. Since the filler length increases with an increasing cross-over arc-length, the transients induced at a layer change would also reduce. Such an approach has been promoted by industry, and the machining capability is available.
- An important feature, influencing the catenary motion, is the location of a layer change with respect to the linear lateral frequencies of the catenary. It is likely that at some stage of the wind linear resonance of the catenary will arise. Since the phase of the lateral excitation reverses after a layer change, it would be advantageous to position the layer change

close to the occurrence of linear resonance. In this manner, the phase of the excitation may be applied to oppose the residual motion which has developed on approaching resonance, dissipating the motion to some extent. This effect is demonstrated in the sensitivity study presented in Appendix L, where a layer change positioned close to the linear resonance reduced the in-plane amplitudes. Although this may be accomplished on existing installations by including additional dead turns on the drum, to allow for fine tuning of the system with regard to the placement of a layer change, due to pulling the *back* end of the rope, and cutting the front end, these locations would not remain constant throughout the life of the rope. Although the simulation results presented in Appendix L demonstrate the potential advantage of a layer change location close to linear resonance, the response is sensitive to the layer change location. Since the layer change location varies during the life of the rope, in practice this would be an unlikely design strategy. Also, reservations exist regarding miscoiling of the rope at a layer change due to the dynamics of the catenary. For this reason Boshoff suggests that the layer change be located away from a linear resonance.

- Since the periodic longitudinal excitation induces compressive pulses in the catenary on the descending cycle, it is more difficult to excite whip; thus it is recommended that if a resonant condition is unavoidable on either the ascending or descending cycle, then it should be accommodated on the descending cycle.

It is worth considering the response amplitudes in the context of the excitation applied to the catenary at the drum. The harmonic amplitudes comprising the out-of-plane excitation are of the order of 7mm and less, whilst those of the longitudinal and in-plane lateral excitation are of the order of 0.1 mm. The amplitude of the in-plane motion is of the order of 1m. This would represent an amplification of 10 000:1 of the in-plane motion. This clearly highlights the importance of the nonlinear coupling in obtaining a realistic simulation of the response.

With reference to the stability analysis presented in chapter 4, a significant region of instability was predicted in the vicinity of a winding speed of 15 m/s, where nonlinear interaction could be expected with regard to the steady state response. This region occurs at approximately 700m, where the second longitudinal mode tuned to the second lateral mode; thus the additive combination resonance involving the second lateral and longitudinal modes is activated by the second harmonic of the Lebus excitation. Simultaneously, the second lateral mode and the second longitudinal mode are directly excited in resonance by the first harmonic of the Lebus coil cross-over frequency. It would be incor-

rect to attempt to assess the dynamic interactions observed in the simulation in terms of the stationary stability analysis, since the system is non-stationary, and steady state amplitudes are not achieved. Also, the transient excitation due to the start-up and the layer change excitation are not accounted for in the stability analysis. Although good experimental correlation was achieved with the laboratory model, and led to an appreciation of parametric excitation, the neglect of the non-stationary aspect of the system compromises the usefulness of the stationary stability analysis of the system as a single design criterion.

The design strategy proposed is thus to apply the stationary stability analysis to identify conditions of resonance, and to develop an appreciation of the overall system tuning. This would be followed by a sensitivity study based on direct numerical simulation, where an overall appraisal of the system response can be obtained. This is still an involved task, and is perhaps better left to a specialist rather than a design engineer.

Chapter 6

Closure

This study presents a non-linear dynamic analysis of a mine hoist system. During the course of this research, studies concerning the dynamics of strings and cables were reviewed, leading to a critical appraisal of the research conducted by Dimitriou and Whillier[1973], and Mankowski[1982]. At the outset of this study, much emphasis was placed on defining practical criteria to design a mine hoist layout, or to correct the adverse dynamic characteristics of an existing installation. This was initially addressed by considering the stationary dynamic behaviour of the system, where the parametric nature of the system could be confirmed on a laboratory model. It is not surprising that although an appreciation of the stationary system characteristics may provide broad guidelines regarding the avoidance of resonance, since the system is non-linear, the non-stationary aspects of the system ultimately exert an overriding influence on the system behaviour. This feature was apparent in the sensitivity study conducted, where the system response was simulated over a range of winding speeds. Nevertheless, the analytical development was correlated with experimental results measured on a laboratory model, providing confidence in the numerical simulation, and allowing design strategies to be suggested. Ultimately, a comprehensive dynamic analysis of a mine hoist system is a complex task, which requires sound engineering judgement tempered with analytical skills. The techniques developed in this thesis are intended to facilitate the latter, without replacing sound engineering judgement.

It is in the interest of further development that a critical appraisal of the current work is provided. This is important for two reasons. Firstly to examine the limitations of the current analysis and to emphasise that substantial scope exists for further development. Secondly to highlight such issues for the benefit of future researchers pursuing similar studies.